Thermochimica Acta 489 (2009) 53–62

Contents lists available at ScienceDirect

Thermochimica Acta

journal homepage: www.elsevier.com/locate/tca

Prediction of solid vapor pressures for organic and inorganic compounds using a neural network

Juan A. Lazzús*

Departamento de Física, Universidad de La Serena, Casilla 554, La Serena, Chile

ARTICLE INFO

Article history:
Received 24 November 2008
Received in revised form 28 January 2009
Accepted 3 February 2009
Available online 13 February 2009

Keywords:
Solid vapor pressure
Artificial neural networks
Property estimation
Thermodynamic properties

ABSTRACT

A method to estimate solid vapor pressures (P^S) for organic and inorganic compounds using an artificial neural network (ANN) is presented. The proposal consists of training an ANN with P^S data of a defined group of substances as a function of temperature, including as learning variable five physicochemical properties to discriminate among the different substances. The following properties were considered: molecular mass, dipole moment, temperature and pressure in the triple point (upper limit of the sublimation curve), and the limiting value $P^S \rightarrow 0$ as $T \rightarrow 0$ (lower limit of the sublimation curve). 152 substances (1520 data points) have been used to train the network. Then, the solid vapor pressures of 60 other solids (600 data points) have been predicted and results compared to experimental data from the literature. The study shows that the proposed method represents an excellent alternative for the estimation of solid vapor pressures and can be used with confidence for any substances.

1. Introduction

The pressure exerted by a vapor in equilibrium with the solid of the same substance is a good definition of solid vapor pressure (P^S). All solids have a tendency to evaporate to a gaseous form so a substance with easily evaporates is referred to as volatile, and the pressure exerted by a vapor in equilibrium with the solid of the same substance is called solid vapor pressure.

A new trend in chemical applications is the use of supercritical solvents either in purifying operations on mixtures of complex pharmaceutical molecules or in stripping on polluted stuff. The optimization of this process can be performed only if the dependence of the solubility both on pressure and temperature can be accurately described and for this purpose, the solid vapor pressure is considered as a key property [1]. This importance of the solid vapor pressure is apparent when writing the equations for the solubility of a solid in the supercritical phase [2]:

$$y_2 = \frac{P_2^S}{P\phi_2} \exp\left[\frac{V_2^S(P - P_2^S)}{RT}\right] \quad (1)$$

This equation is derived from the equifugacity condition between the solid and the fluid phase, under the assumptions that the solubility of the solvent in the solid phase is negligible, the solid is incompressible and the saturated vapor of the pure solid solute at sublimation behaves like an ideal gas. P_2^S is the solid vapor pressure of the pure substance, V_2^S is the solid molar volume, all at the temperature T and φ_2 is the fugacity coefficient of solid at the pressure P.

The solid vapor pressure is relatively small as compared to vapor pressures of liquids at room temperature. However, although small, the solid vapor pressure is needed in applications such as extraction of solids, in particular substances of biological origin, using high pressure gases [3,4]. Considering the valuable information which may be derived either directly or indirectly from sublimation data, it is rather surprising that there is so little quantitative information available in the literature on the sublimation process [5]. In addition, experimental techniques cannot in many cases be used to accurately obtain the solid vapor pressure [6–8].

For some substances, generalized correlations based on the molecular mass (M) and the melting temperature (T_f) have been proposed [9]. Also, to directly estimate the solid vapor pressure, extrapolation of Antoine type equations have been used by Iwai et al. [10] and by Trabelsi et al. [11], while the Lee-Kesler equation have been employed by Nanping et al. [12]. Group contribution methods were applied by Coutsikos et al. [2] for predicting the vapor pressures of a variety of organic solids. Goodman et al. [13] obtained solid vapor enthalpy from functional groups and molecular parameters. From these data they obtained solid vapor pressure using the Clausius–Clapeyron equation. Some researchers have estimated the solid vapor pressure of solid from solubility data [14–17]. Nanping et al. [12] proposed an equation for the solid vapor pressure at a given temperature in terms of the vapor pressure of the gas over the liquid, the solid vapor enthalpy and the melting temperature. Neau et al. [1] proposed to estimate the solid vapor pressure using the Peng–Robinson equation of state.

---

* Tel.: +56 51 204128; fax: +56 51 206658.
E-mail address: jlazzus@dfuls.cl.

0040-6031/$ – see front matter © 2009 Elsevier B.V. All rights reserved.
doi:10.1016/j.tca.2009.02.001

Nomenclature

ANN	artificial neural network
b	bias of the neurons
$f(N)$	transfer function of the neural network
M	molecular weight
N	inputs of the neural network
P^S	solid vapor pressure
P_{TP}	triple point pressure
T	absolute temperature
T_f	melting temperature
T_{TP}	triple point temperature
w	weight of the neural network
y	output of the neural network
Greek letters	
Δ	deviation
μ	dipole moment
Subscripts	
calc	calculated value
lit	literature value

Property estimation procedures are very important in the physico-chemical field for development of mathematical models, since design, optimization and advanced control of processes depend on model parameter values obtained from experimental data. The relationship between the physical and thermodynamic properties is highly non-linear, and consequently an artificial neural network (ANN) can be a suitable alternative to model the underlying thermodynamic properties [18].

Although much has been written and published on the basics of artificial neural network (ANN) and on applications to a variety of problems. The use of ANN to correlate and predict properties such as boiling point, critical temperature, critical pressure, vapor pressure, heat capacity, enthalpy of solid vapor, heat of vaporization, and density, among others, have been thoroughly reviewed by Taskinen and Yliruusi [19]. However, no mention about solid vapor pressure predictions is done by these authors and more recent literature shows no applications on this.

In the method developed in this work, solid vapor pressure data at several temperatures (T) were used to train a neural network. To distinguish between the different substances considered in this study, so the net can discriminate and learn in optimum form, the following properties were used: the molecular mass M (size), the dipole moment μ in debye (polarity), the triple point temperature T_{TP} in Kelvin and the triple point pressure P_{TP} in Pascal (upper end of the solid vapor pressure curve), and the limiting value $P^S \to 0$ as $T \to 0$ (lower end of the solid vapor pressure curve).

2. Computational method

Many models of neural networks have been used in the estimate of thermodynamic properties [18–22]. In this work a feedforward backpropagation neural network was used, which is very effective to represent non-linear relationships among variables. The network programmed with the software Matlab, consists on a multilayer network, in which the flow of information spreads forward through the layers while the propagation of the error is back. In this process, the network uses some factors called "weights" (w_i) to quantify the influence of each fact and of each variable. There are two main states in the operation of a neural network: the learning and the validation. The learning or training is the process for which a neural network modifies the weights in answer to an entrance information [18].

The steps to calculate the output parameter (P^S), using the input parameters, are the following ones:

The net inputs are calculated (N) for the hidden neurons coming from the inputs neurons. For a hidden neuron:

$$N_j^h = \sum_i^n w_{ij}^h p_i + b_j^h \qquad (2)$$

where the p corresponds to the vector of the inputs of the training, j is the hidden neuron, w_{ij} is the weight of the connection among the input neurons with the hidden layer, and the term b_j corresponds to the bias of the neuron j of the hidden layer, reached in its activation. Starting from these inputs the outputs are calculated (y) of the hidden neurons, using a transfer function f^h associated to the neurons of this layer.

$$y_j^h = f_j^h \left(\sum_i^n w_{ij}^h p_i + b_j^h \right) \qquad (3)$$

Similar calculations are carried out to obtain the results of each neuron of the following layer until the output layer.

To minimize the error the transfer function f it should be differentiable. In the net two types of transfer function were used: the lineal function $f(N_{jk}) = (N_{jk})$ and the hyperbolic tangent function (tansig) defined by the equation:

$$f(N_{jk}) = \frac{e^{N_{jk}} - e^{-N_{jk}}}{e^{N_{jk}} + e^{-N_{jk}}} \qquad (4)$$

All the neurons of the network have an associate activation value for a given input pattern, the algorithm continues finding the error that is presented for each neuron, except those of the input layer. After finding the value of the gradient of the error the weights of network are actualized, for all layers.

This process repeats for the total number of patterns to training, for a successful process the objective of the algorithm is to modernize all the weight and bias of the neural network minimizing the total mean squared error. Fig. 1 presents a block diagram of the program developed.

The most basic architecture normally used for this type of application involves a feed-forward backpropagation neural network consisting of three or four layers [19]. There is no specific approach to determine the number of neurons of the hidden layer, many alternative combinations are possible. The optimum number of neurons was determined by adding neurons in systematic form and evaluating the average absolute deviations of the sets during the learning process. Fig. 2 shows this methodology.

3. Database used

In this study, 1520 data points of 152 substances (10 points for each substances), were used to train the network and then values of solid vapor pressures of 60 substances (600 data points), not used in the training process, were predicted. To distinguish between the different substances considered in this study, so the net can discriminate and learn in optimum form, the following properties were used: molecular mass M (size), dipole moment μ in debye (polarity), the triple point temperature T_{TP} in Kelvin and the triple point pressure P_{TP} in Pascal (upper end of the sublimation curve), and the limiting value $P^S \to 0$ as $T \to 0$ (lower end of the sublimation curve). This last condition adds an interesting desirable condition for the network to learn and has been discussed in detail by Diu et al. [23], based on purely thermodynamic grounds these authors showed that the solid vapor curve reaches the origin in the T–P^S plane, with a quasi-universal behavior. In other works based on

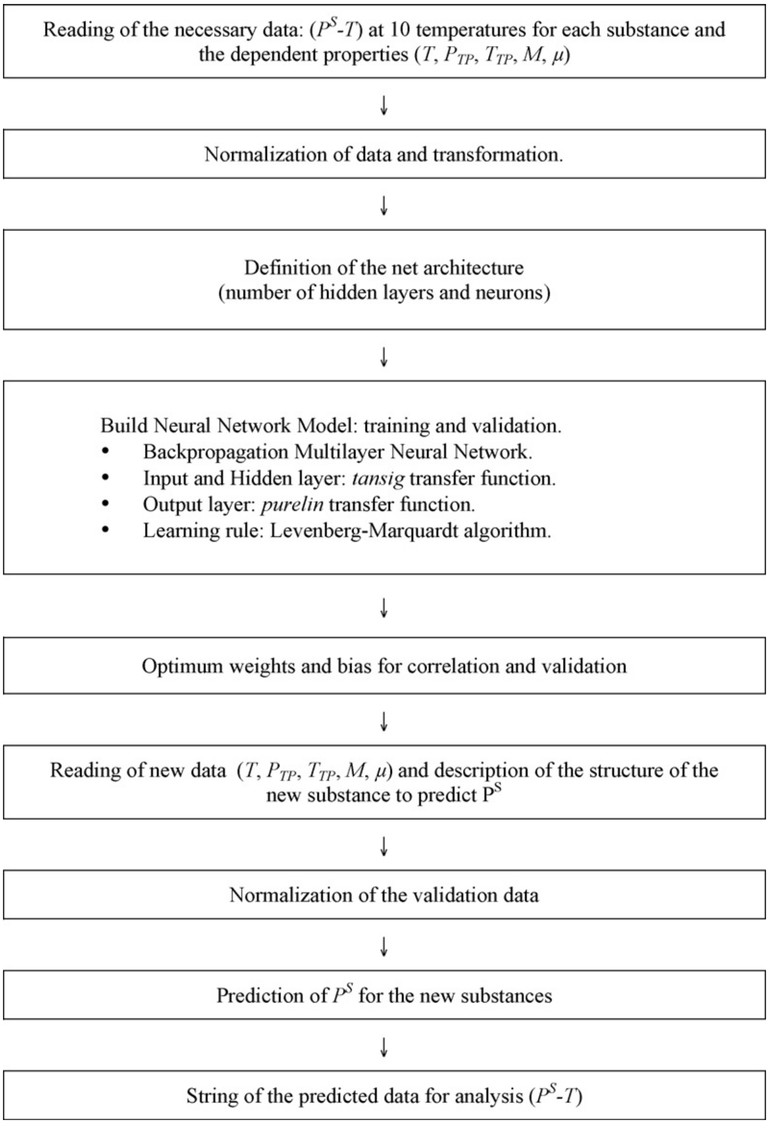

Fig. 1. Flow diagram for the ANN program developed for this work.

neural networks, the inclusion of the dipole moment proved to be particularly useful in distinguishing isomers [21,22]. All the input parameters were selected arbitrarily. Molecular mass and dipole moment were chosen to characterize the different molecules. The molecular mass has been used previously to estimate sublimation properties [9]. The dipole moment has been used to predict vapor pressure [24]. Both properties have also been used recurrently in applications QSPR [25]. The other properties were used to characterize the sublimation curve of each substance [1,13,23]. All 212 substances (163 organics and 49 inorganics), and the properties of interest (M, μ, T_{TP}, P_{TP}) are listed in Table 1. This table also shows the range of temperature and the range of solid vapor pressure of the data used. These values are of especial importance to verify that an acceptable range of temperature is covered in the study and to see the order of magnitude of the solid vapor pressure. In other works for estimating the solid vapor pressure [1,2], the authors compare their models with a great number of experimental data points for different substances. The problem is that the reliability of these experimental data is never established. Uncertainties are not given for any of the experimental data, which makes it impossible to interpret the deviations between the models and the experimental data. This is especially troubling given the history of unreliable experimental data that have been collected for the sublimation curve [5]. It would be much more useful and productive to select only the best experimental data sets (with well established uncertainties), and to use these data sets to develop and test models. In this work the data were taken from different sources: all the properties of interest (M, μ, T_{TP}, P_{TP}) and the solid vapor pressure data of 179 substances were taken from the DIPPR database [26] that includes estimated uncertainties for the experimental data, and only for 33 substances the solid vapor pressure data were taken from the Handbook of Chemistry and Physics [27], that has been used for similar applications [2,28]. Only ten values that cover the total range of the solid vapor pressure of each substance were taken from ranges published in these databases [26,27].

As seen in Table 1 both the temperature and the solid vapor pressure cover wide ranges, going from 11 to 4000 (K) and 0.001 to ≈4000000 (Pa). Examples of this wide range of temperatures and pressures that the ANN must treat for training and prediction are the high values of solid vapor pressure (325–100000 Pa) at low temperatures (130–192 K) for acetylene; or at high temperatures (1728–2175 K) and low pressures (0.002–2.5 Pa) for vanadium; or

Table 1
Substances and properties used in the Neural Network model and deviations during training and prediction.

Substance			Properties[a]						Deviations			
No.	Formula	Name	M	μ (D)	T_{TP} (K)	P_{TP} (Pa)	ΔT^S (K)	ΔP^S (Pa)	$\%\Delta P^S_{min}$	$\%\Delta P^S_{max}$	$\%\Delta P^S$	$\|\%\Delta P^S\|$
Training set												
1	Ag	Silver	107.9	0.000	1234.0	0.2	1034–1224	0.001–0.2	2.3	11.4	0.2	6.1
2	$AlCl_3$	Aluminum chloride	133.3	2.030	465.7	233000.0	373–466	137–228750	1.3	14.5	0.4	7.1
3	AsH_3	Arsine	77.9	0.201	156.2	2985.2	131–155	134–2679	0.5	19.0	−1.8	8.2
4	Br2	Bromine	159.8	0.000	265.9	5853.4	169–266	0.05–6277	0.2	7.3	1.1	3.8
5	C	Carbon	12.0	0.000	4530.0	10436000.0	2300–4000	0.002–53204	0.1	4.7	0.1	2.5
6	Ca	Calcium	40.1	0.000	1115.0	208.9	700–1112	0.003–201	0.0	4.6	−0.1	2.3
7	CF_4	Carbon tetrafluoride	88.0	0.000	89.6	109.0	76–90	2.9–108	1.4	9.9	0.1	4.6
8	CH_3I	Iodide, methyl	141.9	1.619	206.7	254.6	176–205[b]	5–199[b]	0.4	4.2	0.0	2.3
9	CH_4	Methane	16.0	0.000	90.7	11696.0	79–89	1710–9294	0.0	5.9	−0.2	2.6
10	CNCl	Cyanogen chloride	61.5	2.820	266.9	44649.0	196–267	133–42693	0.5	3.5	0.2	2.0
11	$C_2Cl_4F_2$	Ethane, 1,1,1,2-tetrachlorodifluoro	203.8	1.391	313.8	16103.0	262–314	1301–17103	0.2	6.1	0.1	2.2
12	C_2Cl_6	Ethane, hexachloro	236.7	0.000	460.0	107000.0	286–447	31–73618	1.2	15.8	0.2	6.3
13	C_2F_6	Ethane, hexafluoro	138.0	0.000	173.1	27054.0	98–169	3.4–10316	1.4	19.2	−2.6	9.3
14	C_2H_2	Acetylene	26.0	0.000	192.4	127450.0	133–187	325–99337	0.9	15.5	0.4	6.3
15	$C_2H_2O_4$	Oxalic acid	90.0	2.629	462.7	2152.3	328–378	0.8–70	0.3	2.6	0.1	1.3
16	C_2H_4	Ethylene	28.1	0.000	104.0	126.0	77–102	0.04–66	0.8	11.8	0.2	4.7
17	$C_2H_4Br_2$	Ethylene dibromide	187.9	1.010	282.9	753.3	252–281	47–543	0.1	3.3	−0.1	1.4
18	$C_2H_4N_4$	Dicyandiamide	84.1	8.214	482.7	5054.9	420–448	0.1–1.0	0.3	2.3	0.0	1.1
19	$C_2H_5NO_2$	Glycine	75.1	12.801	509.4	304.8	408–431	0.1–1.2	0.8	6.9	0.0	3.7
20	C_2H_6	Ethane	30.1	0.000	90.4	1.1	81–89	0.05–0.8	1.9	22.7	0.3	12.7
21	$C_3H_2N_2$	Malononitrile	66.1	3.717	305.0	19.7	256–305	0.1–23	0.0	14.7	0.3	6.8
22	C_3H_4	Propadiene	40.1	0.000	136.9	18.3	110–137	0.04–18	0.0	0.9	0.1	0.4
23	$C_3H_4N_2$	Pyrazole	68.1	2.215	341.7	1350.6	253–313	26–4412	0.5	16.3	0.4	8.1
24	C_4F_8	Cyclobutane, octafluoro	200.0	0.000	233.0	19034.0	177–233	643–18670	2.7	23.5	4.9	11.2
25	$C_4H_{10}O$	2-Propanol, 2-methyl	74.1	1.670	299.0	5884.3	253–298	134–5455	0.3	5.1	0.3	2.0
26	$C_4H_2N_2$	Fumaronitrile	78.1	0.000	369.7	3972.5	245–281	0.1–5	0.5	19.0	−0.4	7.6
27	$C_4H_2O_3$	Maleic anhydride	98.1	3.927	325.7	289.8	308–325	48–292	0.2	14.4	0.2	5.2
28	$C_4H_4N_2$	Pyrazine	80.1	0.240	327.2	10847.0	288–327	657–11229	0.3	6.3	0.9	3.5
29	$C_4H_4N_2$	Succinonitrile	80.1	3.927	331.2	12.0	279–298	0.1–1.0	0.4	4.1	0.1	1.9
30	$C_4H_4O_3$	Succinic anhydride	100.1	3.830	393.0	862.8	365–388	133–667	0.2	3.7	0.0	1.6
31	C_4H_4S	Thiophene	84.1	0.540	234.9	185.6	193–235	1.4–189	0.4	4.4	0.1	2.1
32	$C_4H_6O_2$	trans-Crotonic acid	86.1	2.129	344.6	807.3	293–343	24–880	0.6	6.3	1.1	3.3
33	C_4H_7NO	Acrylamide, 2-metha	85.1	3.133	383.7	2825.1	325–375	14–905	0.3	3.0	0.1	1.2
34	C_4H_8	Cyclobutane	56.1	0.000	182.5	180.1	181–214[b]	131–2795[b]	1.4	9.3	0.5	5.2
35	$C_5H_8N_4O_{12}$	Pentaerythritol tetranitrate	316.1	2.479	413.7	339.5	370–411	0.08–10	0.5	3.3	0.1	1.3
36	$C_5H_8O_4$	Glutaric acid	132.1	2.641	370.1	1.8	292–320	292–320	0.3	4.7	0.1	1.7
37	$C_5H_{12}O_2$	Neopentyl glycol	104.1	2.698	403.3	5267.3	338–401	158–3301	0.0	3.7	0.0	1.7
38	$C_5H_{12}O_4$	Pentaerythritol	136.1	2.009	538.7	2216.0	379–408	0.02–0.7	0.1	3.8	−0.1	1.6
39	C_6F_6	Benzene, hexafluoro	186.1	0.330	278.3	3931.0	216–269	9–1936	0.8	13.0	0.2	5.1
40	$C_6H_3Cl_3$	Benzene, 1,2,3-trichloro	181.4	2.440	325.7	183.0	289–303	8–27	0.3	7.1	0.1	3.4
41	$C_6H_3Cl_3$	Benzene, 1,3,5-trichloro	181.4	0.309	336.7	651.8	282–301	7–31	0.9	25.1	2.0	12.5
42	$C_6H_3N_3O_6$	Benzene, 1,3,5-trinitro	213.1	0.411	398.4	8.5	359–387	0.6–7	0.4	6.1	0.1	2.6
43	$C_6H_4N_2O_4$	Benzene, o-dinitro	168.1	6.296	390.1	108.4	343–391	0.3–13	0.1	7.9	0.5	3.2
44	$C_6H_4N_2O_4$	Benzene, m-dinitro	168.1	3.837	363.2	30.2	332–361	0.3–3	0.0	1.6	0.0	0.5
45	$C_6H_4N_2O_4$	Benzene, p-dinitro	168.1	0.000	446.6	3045.0	339–398	0.08–11	0.4	21.1	−2.0	9.4
46	$C_6H_4O_2$	Quinone	108.1	0.000	388.9	11651.0	250–388	0.1–11234	0.3	7.8	0.9	4.2
47	C_6H_6ClN	Aniline, p-chloro	127.6	2.989	343.1	218.9	290–332	1.3–133	0.0	5.4	0.1	2.2
48	$C_6H_6O_2$	Benzene, 1,4-dihydroxy	110.1	1.781	444.7	2229.7	341–400	0.4–91	1.9	16.9	−1.7	7.1
49	$C_6H_6O_2$	Hydroquinone	110.1	1.781	444.7	2229.7	406–437[b]	138–1417[b]	0.7	3.8	1.7	1.7
50	C_6H_7N	Pyridine, 3-methyl	93.1	2.401	255.0	34.7	228–255	1–33	0.1	5.9	0.1	2.1
51	C_6H_7N	Pyridine, 4-methyl	93.1	2.581	276.8	186.5	230–257	10–316	0.4	7.3	0.2	4.0
52	$C_6H_8N_2$	Benzene, 1,2-diamino	108.1	1.529	377.0	338.4	298–373	1.6–326	0.5	10.4	2.2	2.9
53	$C_6H_8N_2$	Benzene, 1,4-diamino	108.1	1.529	413.0	1388.2	298–373	0.5–144	0.1	10.6	−0.9	4.4
54	$C_6H_{10}O_4$	Adipic acid	146.1	2.320	425.5	78.1	359–406	0.06–9	0.2	12.3	0.0	5.4
55	$C_6H_{11}NO$	ε-Caprolactam	113.2	3.867	342.3	39.8	294–314	0.1–1.4	1.1	12.8	0.2	5.0
56	C_6H_{12}	Cyclohexane	84.2	0.000	279.7	5362.5	268–278	2699–4935	0.7	11.3	−3.6	5.1
57	$C_6H_{12}N_4$	Formamine	140.2	0.860	553.2	99745.0	298–453	0.1–2675	0.1	9.0	0.4	2.6
58	$C_6H_{12}O$	Cyclohexanol	100.2	1.859	296.6	76.5	269–298	7–93	0.8	14.8	0.7	7.5
59	C_6H_{14}	Hexane	86.2	0.000	177.8	1.0	168–178	0.1–1	0.5	23.9	−0.7	12.9
60	$C_7H_6N_2O_4$	Toluene, 2,4-dinitro	182.1	4.317	342.7	7.9	277–344	0.002–5	0.5	4.9	0.1	3.0
61	$C_7H_6N_2O_4$	Toluene, 2,6-dinitro	182.1	2.809	337.9	25.0	277–323	0.004–1.8	0.1	13.0	0.2	4.5
62	$C_7H_6O_2$	Phenol, p-formyl	122.1	3.957	390.2	106.7	312–337[b]	0.04–0.6[b]	0.4	16.4	0.4	5.5
63	C_7H_8O	o-Cresol	108.1	1.451	304.2	65.3	276–304	3.2–72	0.2	12.3	−3.0	5.3
64	C_7H_8O	m-Cresol	108.1	1.589	285.4	5.9	273–285	2–6	1.8	26.2	1.7	12.8
65	C_7H_8O	p-Cresol	108.1	1.559	307.9	34.5	278–308	2–41	0.4	24.6	4.7	7.6
66	$C_7H_8O_2$	Phenol, p-methoxy	124.1	1.919	328.7	11.5	278–300	0.04–0.7	0.9	10.5	−0.7	5.0
67	$C_7H_{12}O_4$	Pimelic acid	160.2	2.389	379.2	1.2	325–379[b]	0.002–1.1[b]	0.7	16.4	0.5	6.3
68	C_7H_{16}	Heptane	100.2	0.000	182.6	0.18	175–179	0.04–0.14	1.6	18.7	1.0	9.2
69	$C_8H_4O_3$	Phthalic anhydride	148.1	5.290	404.2	790.0	303–333	0.1–2.9	1.0	6.0	0.2	3.2
70	$C_8H_6O_4$	Isophthalic acid	166.1	2.269	619.2	2820.7	493–563	95–2969	0.3	5.3	0.2	1.5
71	$C_8H_6O_4$	Terephthalic acid	166.1	2.434	700.2	4574.9	523–675	98–92669	0.1	8.1	0.0	3.8
72	$C_8H_8O_2$	Phenol, p-acetyl	136.2	3.777	382.2	22.0	320–348[b]	0.05–0.9[b]	0.2	4.9	0.2	1.9
73	C_8H_9NO	Acetanilide	135.2	4.047	387.7	118.3	303–324	0.03–0.2	0.6	8.5	0.2	3.3

Table 1 (*Continued*)

Substance			Properties[a]						Deviations			
No.	Formula	Name	M	μ (D)	T_{TP} (K)	P_{TP} (Pa)	ΔT^S (K)	ΔP^S (Pa)	$\%\Delta P^S_{min}$	$\%\Delta P^S_{max}$	$\%\Delta P^S$	$\lvert\%\Delta P^S\rvert$
74	C_8H_{10}	p-Xylene	106.2	0.000	286.4	575.5	247–286	12–546	1.1	14.1	−1.7	4.6
75	$C_8H_{10}N_4O_2$	Caffeine	194.2	3.687	509.2	4751.0	446–509	117–4715	1.0	8.4	0.1	3.9
76	$C_8H_{10}O$	Phenol, p-ethyl	122.2	1.781	318.2	46.0	262–316	0.04–30	0.6	5.6	0.2	2.8
77	$C_8H_{10}O$	Phenol, 2,3-dimethyl	122.2	1.250	345.7	362.0	265–343	0.05–314	0.9	5.6	−0.2	2.4
78	$C_8H_{10}O$	Phenol, 2,5-dimethyl	122.2	1.430	348.0	561.2	264–347	0.04–500	0.5	11.6	−1.0	5.5
79	$C_8H_{10}O$	Phenol, 2,6-dimethyl	122.2	1.409	318.8	165.3	248–317	0.05–150	0.1	3.4	0.7	1.7
80	$C_8H_{10}O$	Phenol, 3,4-dimethyl	122.2	1.769	338.3	115.4	270–337	0.05–100	2.6	25.1	10.2	12.5
81	$C_8H_{10}O$	Phenol, 3,5-dimethyl	122.2	1.760	336.6	119.7	267–334	0.05–100	5.9	17.5	−9.5	9.5
82	C_8H_{18}	Butane, 2,2,3,3-tetramethyl	114.2	0.000	374.0	86930.0	252–340	97–22992	3.5	24.8	0.5	12.6
83	$C_9H_8O_4$	Acetylsalicylic acid	180.2	2.090	408.2	280.4	313–364[b]	0.02–7[b]	0.7	17.1	−2.0	7.8
84	$C_9H_{16}O_4$	Nonanedioic acid	188.2	2.350	379.7	0.5	330–379[b]	0.002–1.1[b]	0.3	15.2	0.2	5.7
85	$C_{10}H_6O_2$	1,4-Naphthoquinone	158.2	0.000	401.5	852.0	310–325[b]	0.2–1.4[b]	0.0	8.8	3.6	3.8
86	$C_{10}H_8$	Naphthalene	128.2	0.000	353.4	991.3	279–294	1.4–7	1.2	3.6	2.6	2.6
87	$C_{10}H_{10}O_4$	Dimethyl terephthalate	194.2	2.188	413.8	1257.7	373–413	62–1162	0.5	7.7	0.2	2.8
88	$C_{10}H_{14}$	Benzene, 1,2,4,5-tetramethyl	134.2	0.000	352.4	1784.8	263–348	0.3–1379	0.2	2.7	−1.0	1.7
89	$C_{10}H_{14}O$	Phenol, p-tert-butyl	150.2	1.619	372.0	496.3	281–303[b]	0.06–0.8[b]	0.2	7.6	0.4	3.0
90	$C_{10}H_{16}$	Adamantane	136.2	0.000	541.2	482000.0	278–443	3–36274	0.0	14.3	0.3	7.2
91	$C_{10}H_{16}O$	Camphor	152.2	3.100	453.3	51396.0	273–453	5–56047	0.3	11.0	0.2	6.0
92	$C_{10}H_{18}O_4$	Sebacic acid	202.3	2.400	407.7	4.2	375–403[b]	0.04–1.6[b]	0.1	3.0	−0.2	1.3
93	$C_{10}H_{20}O_2$	Capric Acid	172.3	1.679	304.6	0.15	289–301	0.01–0.1	1.5	14.8	0.3	7.9
94	$C_{11}H_{10}$	Naphthalene, 2-methyl	142.2	0.420	307.7	18.7	283–308	2–18	2.6	25.2	0.9	12.3
95	$C_{11}H_{16}$	Benzene, pentamethyl	148.2	0.069	327.5	113.0	296–313	7–38	0.6	12.0	2.7	4.5
96	$C_{12}H_8O$	Dibenzofuran	168.2	0.881	355.3	76.6	299–346	0.5–36	1.5	24.1	0.2	7.6
97	$C_{12}H_{10}$	Acenaphthene	154.2	0.255	366.6	200.0	291–310	0.1–1.1	0.1	26.4	11.8	11.8
98	$C_{12}H_{10}N_2O_2$	Diphenylamine, p-dinitro	214.2	5.996	408.6	128.3	382–403	0.2–2	0.1	3.1	0.1	1.2
99	$C_{12}H_{11}N$	Diphenylamine	169.2	1.079	326.2	3.0	298–324	0.09–1.6	0.0	3.0	0.2	1.0
100	$C_{12}H_{12}$	Naphthalene, 2,7-dimethyl	156.2	0.411	368.8	375.0	333–368	20–360	1.2	21.6	1.4	9.6
101	$C_{12}H_{12}$	Naphthalene, 2,6-dimethyl	156.2	0.140	383.3	783.0	279–383	0.03–773	1.7	24.7	−7.8	14.0
102	$C_{12}H_{18}$	Benzene, hexamethyl	162.3	0.070	438.7	6141.8	289–364	0.04–40	0.9	21.0	1.5	6.6
103	$C_{13}H_9N$	Acridine	179.2	2.150	383.2	37.2	302–343	0.01–0.8	3.1	25.8	−1.8	12.1
104	$C_{13}H_{10}$	Fluorene	166.2	0.249	387.9	281.7	306–322	0.2–1.1	1.5	17.0	1.0	8.1
105	$C_{13}H_{12}$	Methane, diphenyl	168.2	0.770	298.4	2.0	274–299	0.13–1.9	0.1	7.7	0.4	3.3
106	$C_{13}H_{26}O_2$	Methyl dodecanoate	214.3	1.700	278.2	0.06	262–273	0.002–0.02	0.2	3.5	0.2	1.6
107	$C_{13}H_{26}O_2$	Tridecanoic acid	214.3	1.649	315.0	0.012	304–312[b]	0.003–0.02[b]	0.6	7.9	0.0	4.2
108	$C_{14}H_{10}$	Anthracene	178.2	0.000	488.9	4950.9	338–353	0.1–0.5	0.4	4.3	0.7	2.3
109	$C_{14}H_{10}$	Phenanthrene	178.2	0.000	372.4	29.3	310–323	0.08–0.33	0.1	3.6	−0.9	1.2
110	$C_{14}H_{12}$	trans-Stilbene	180.2	0.000	397.4	233.6	318–365	0.1–12	0.7	11.8	1.9	6.1
111	$C_{14}H_{14}$	Bibenzyl	182.3	0.455	324.3	8.8	286–307	0.1–1.1	0.3	15.3	−0.8	8.4
112	$C_{14}H_{28}O_2$	Myristic acid	228.4	1.679	327.4	0.026	311–325	0.003–0.03	0.0	0.9	0.2	0.4
113	$C_{14}H_{30}$	Tetradecane	198.4	0.000	279.0	0.25	268–276	0.04–0.14	0.8	16.6	0.4	8.1
114	$C_{14}H_{30}O$	Tetradecanol	214.4	1.550	310.7	0.08	293–307	0.002–0.03	0.1	4.4	0.0	2.2
115	$C_{15}H_{30}O_2$	Pentadecanoic acid	242.4	1.721	325.7	0.008	313–321[b]	0.001–0.01[b]	0.2	3.5	−0.1	1.9
116	$C_{16}H_{32}O_2$	Palmitic acid	256.4	1.739	335.7	0.013	319–333	0.001–0.01	0.9	14.3	0.7	7.5
117	$C_{16}H_{34}$	Hexadecane	226.4	0.000	291.3	0.09	282–290	0.02–0.08	1.3	18.5	0.4	8.7
118	$C_{16}H_{34}O$	Hexadecanol	242.4	1.670	322.4	0.045	308–320	0.003–0.03	1.3	13.1	0.3	7.0
119	$C_{17}H_{34}O_2$	Heptadecanoic acid	270.5	1.691	334.3	0.006	326–331[b]	0.001–0.003[b]	0.2	3.0	−0.2	1.5
120	$C_{17}H_{36}$	Heptadecane	240.5	0.000	295.1	0.047	288–293	0.01–0.028	0.1	2.4	0.2	1.1
121	$C_{18}H_{12}$	Naphthacene	228.3	0.000	630.2	18421.0	421–449	0.1–1	0.6	6.1	0.0	2.5
122	$C_{18}H_{14}$	o-Terphenyl	230.3	0.103	329.4	0.41	323–333	0.3–0.7	1.2	12.5	0.4	6.4
123	$C_{18}H_{30}$	Benzene, hexaethyl	246.4	0.000	403.2	288.0	298–323	2–2669	1.0	12.6	0.2	5.1
124	$C_{18}H_{38}$	n-Octadecane	254.5	0.000	301.3	0.034	288–298	0.002–0.01	0.4	4.9	0.1	2.6
125	$C_{18}H_{38}O$	Octadecanol	270.5	1.661	331.1	0.025	320–329	0.003–0.02	0.1	4.9	0.3	2.7
126	$C_{19}H_{16}$	Methane, triphenyl	244.3	0.210	365.3	3.7	325–349	0.05–0.64	0.1	1.4	0.3	0.7
127	$C_{19}H_{38}O_2$	Nonadecanoic acid	298.5	1.649	341.2	0.002	337–341[b]	0.001–0.0034[b]	0.8	8.3	0.2	4.5
128	$C_{19}H_{40}$	Nonadecane	268.5	0.000	305.0	0.016	291–303	0.001–0.01	0.3	4.3	0.1	1.7
129	$C_{20}H_{40}O_2$	Arachidic acid	312.5	1.670	348.2	0.004	341–348	0.001–0.004	0.1	3.4	0.0	1.7
130	$C_{20}H_{42}O$	Eicosanol	298.6	1.829	338.6	0.01	327–337	0.001–0.01	0.1	2.0	0.0	0.9
131	$C_{26}H_{22}$	Ethane, 1,1,2,2-tetraphenyl	334.5	0.000	485.2	1672.0	364–423	0.004–2	0.1	10.1	0.1	4.7
132	$C_{40}H_{56}$	β-Carotene	536.9	0.000	706.2	81.0	520–700	0.002–62	0.1	3.2	−0.1	1.5
133	F_2	Fluorine	38.0	0.000	53.5	252.0	32–53	0.05–269	0.2	6.7	−0.2	1.8
134	$FeCl_3$	Ferric chloride	162.2	1.280	577.0	77743.0	425–575	3–67952	0.5	20.1	−1.5	10.4
135	GaC_3H_9	Gallium, trimethyl	114.8	0.000	257.5	3341.0	247–257[b]	1342–3159[b]	1.2	11.5	0.3	6.0
136	H_2	Hydrogen	2.0	0.000	14.0	7220.0	12–14	1333–7993	0.1	4.4	−0.2	2.2
137	H_2O	Water	18.0	1.850	273.2	611.7	172–273	0.001–614	0.3	1.6	−0.1	0.8
138	H_2Se	Hydrogen selenide	81.0	0.240	207.5	27400.0	173–210	1359–33634	0.5	7.4	−0.5	2.7
139	I_2	Iodine	253.8	0.000	386.8	12210.0	237–387	0.05–12104	0.6	19.9	0.6	10.1
140	KCl	Potassium chloride	74.6	10.271	1044.0	48.9	750–877	0.002–0.3	1.0	5.8	0.1	3.1
141	KI	Potassium iodide	166.0	9.234	954.0	35.7	722–898	0.02–17	0.9	5.0	0.1	2.9
142	N_2O	Nitrous oxide	44.0	0.167	182.3	87850.0	130–179	132–64738	0.3	11.5	0.0	5.2
143	N_2O_4	Nitrogen tetroxide	92.0	0.000	261.9	18559.0	234–263	1333–19993	0.8	9.5	2.9	4.9
144	Ne	Neon	20.2	0.000	24.6	43300.0	16–25	72–43497	2.4	24.5	−4.1	15.3
145	$NOCl$	Nitrosyl chloride	65.5	1.901	213.6	5437.7	176–216	128–6665	0.0	5.7	0.1	1.8
146	O_3	Ozone	48.0	0.540	80.2	0.7	66–80	0.001–0.7	0.3	19.1	0.2	7.3
147	P	Phosphorus	31.0	0.000	863.2	4400000.0	510–863	133–4387500	0.6	2.8	0.0	1.6

Table 1 (*Continued*)

Substance			Properties[a]						Deviations			
No.	Formula	Name	M	μ (D)	T_{TP} (K)	P_{TP} (Pa)	ΔT^S (K)	ΔP^S (Pa)	$\%\Delta P^S_{min}$	$\%\Delta P^S_{max}$	$\%\Delta P^S$	$\|\%\Delta P^S\|$
148	PCl_5	Phosphorus pentachloride	208.2	0.000	433.2	102730.0	351–432	1306–99433	0.5	20.2	0.8	10.7
149	P_4O_{10}	Phosphorus pentoxide	283.9	0.000	693.2	486010.0	523–693[b]	2278–479730[b]	0.3	6.7	−0.1	2.6
150	SiO_2	Silicon dioxide	60.1	0.579	1696.0	19.8	1273–1473	0.001–0.01	0.2	4.0	−0.1	2.0
151	SO_3	Sulfur trioxide	80.1	0.000	290.0	21130.0	234–293	133–26528	1.3	21.8	1.9	11.0
152	V	Vanadium	50.9	0.000	2190.0	3.1	1728–2175	0.002–2.5	0.8	8.4	0.3	4.7
Predicted set												
153	As	Arsenic	74.9	0.000	1095.2	3698400.0	480–1088	0.007–3221000	0.3	4.3	0.3	2.1
154	As_2O_3	Arsenic trioxide	197.8	0.130	551.0	4131.5	400–583	0.7–8433	0.7	13.1	0.2	4.2
155	BF_3	Boron trifluoride	67.8	0.000	144.8	8340.0	119–145	132–8488	0.4	6.5	−0.4	3.3
156	BrH	Hydrogen bromide	80.9	0.821	185.2	29890.0	135–185	100–27400	1.1	23.3	0.9	9.9
157	CCl_4	Carbon tetrachloride	153.8	0.000	250.3	1122.5	209–225	33–160	0.0	4.7	−1.2	2.0
158	CHN	Hydrogen cyanide	27.0	2.980	259.8	18625.0	200–260	200–18620	1.0	13.4	0.4	6.1
159	CH_2O_2	Formic acid	46.0	1.415	281.5	2402.4	268–281	660–2319	3.4	23.2	−1.9	12.3
160	CH_4N_2O	Urea	60.1	4.557	405.9	93.13	341–368	0.1–1.3	0.5	5.1	0.2	2.6
161	ClH	Hydrogen chloride	36.5	1.079	159.0	13522.0	120–159[b]	100–13500[b]	0.7	12.6	0.7	5.1
162	CO	Carbon monoxide	39.9	0.000	83.8	68700.0	50–68	100–15400	0.3	27.4	−4.3	11.1
163	CO_2	Carbon dioxide	44.0	0.000	216.6	518670.0	130–217	32–518000	2.5	11.1	0.3	5.8
164	$C_2H_4O_2$	Acetic acid	60.1	1.739	289.8	1276.9	238–283[b]	30–857[b]	0.8	7.7	0.3	4.0
165	C_2H_5NO	Acetamide	59.1	3.747	353.3	336.4	298–350[b]	2.4–251[b]	0.1	4.8	0.1	2.2
166	C_2N_2	Cyanogen	52.0	0.000	245.3	73807.0	180–245	230–74470	1.2	18.5	−0.2	8.1
167	$C_3H_6O_3$	Trioxane	90.1	2.081	334.7	14429.0	298–311	1694–4161	1.0	15.2	−0.5	8.3
168	$C_4H_4Cl_2$	Benzene, p-dichloro	147.0	0.000	326.1	1225.0	283–323[b]	31–1141[b]	0.6	7.3	−1.2	3.8
169	C_4H_6	Acetylene, dimethyl	54.1	3.957	240.9	6121.2	227–241	1989–6218	0.1	4.7	0.2	1.6
170	C_4H_6O	Succinic acid	118.1	2.200	460.7	884.9	372–401	0.5–8	0.3	8.9	0.2	4.8
171	$C_4H_6O_6$	Tartaric Acid	150.1	3.627	479.2	14.4	315–330[b]	0.2–2[b]	0.4	5.8	0.1	2.9
172	$C_5H_{10}O_2$	Neopentanoic acid	102.1	1.700	309.1	144.4	242–257	0.1–1	1.7	21.6	−3.0	11.2
173	C_5H_{12}	Neopentane	72.2	0.000	256.6	35745.0	221–255	3993–33268	1.0	18.8	1.0	9.9
174	C_6Cl_6	Benzene, hexachloro	284.8	0.540	501.7	10201.0	388–502	133–10523	0.0	12.4	0.1	5.2
175	$C_6H_3Cl_3$	Benzene, 1,2,4-trichloro	181.4	1.260	290.2	33.1	279–298	8–45	1.3	19.3	0.8	10.4
176	$C_6H_4ClNO_2$	Benzene, p-chloro-1-nitro	157.6	2.830	356.7	243.8	273–305	0.1–7	0.2	2.0	0.0	0.8
177	$C_6H_5NO_2$	Benzene, 1-nitro	123.1	4.227	278.9	6.69	243–273	0.1–4	0.5	12.9	0.3	5.6
178	C_6H_6	Benzene	78.1	0.000	278.7	4764.2	243–278	294–4624	0.3	9.7	2.4	5.4
179	C_6H_6O	Phenol	94.1	1.451	314.1	188.0	278–305	6–87	1.7	20.6	−0.2	10.0
180	$C_6H_{12}N_2$	Triethylenediamine	112.2	3.358	434.3	69669.0	323–373	522–7636	0.3	8.0	0.2	2.8
181	$C_7H_5N_3O_6$	Toluene, 2,4,6-trinitro	227.1	1.160	354.0	0.94	323–416	0.02–406	0.1	4.7	0.2	1.8
182	$C_7H_6O_2$	Benzoic acid	122.1	1.001	395.5	795.5	343–387[b]	12–451[b]	0.2	2.4	−0.4	1.1
183	$C_7H_6O_3$	Salicylic acid	138.1	2.650	431.8	2802.7	368–407	30–596	0.2	3.8	0.1	1.3
184	C_8H_7N	Indole	117.2	2.081	326.2	31.5	283–323	0.4–14	1.7	16.4	0.7	7.8
185	$C_8H_8O_3$	Vanillin	152.2	2.869	355.0	11.8	298–355[b]	0.03–13[b]	0.2	4.2	0.2	1.6
186	$C_8H_{14}O_4$	Suberic acid	174.2	2.359	416.2	22.2	379–407[b]	0.2–5[b]	0.6	9.9	0.2	4.0
187	$C_{10}H_{14}O$	Thymol	150.2	1.619	323.0	37.2	273–313[b]	0.07–13[b]	0.9	8.0	−0.2	3.0
188	$C_{12}H_8$	Acenaphthylene	152.2	0.300	362.7	170.0	273–373	0.08–347	0.3	21.2	−6.0	12.1
189	$C_{12}H_{10}$	Biphenyl	154.2	0.000	342.2	94.2	279–299	0.13–1.1	0.3	2.7	−1.0	1.8
190	$C_{12}H_{24}O_2$	Lauric acid	200.3	1.640	317.0	0.04	295–314	0.002–0.05	0.4	10.3	0.4	4.7
191	$C_{13}H_{10}O$	Benzophenone	182.2	2.980	321.4	1.5	289–315[b]	252–6603[b]	0.2	3.3	0.1	1.6
192	$C_{14}H_8O_2$	Anthraquinone	208.2	0.000	559.2	12846.0	497–559	734–14068	0.4	4.2	0.0	2.3
193	$C_{14}H_{22}$	Benzene, 1,4-di-tert-butyl	190.3	0.579	350.8	295.9	285–325	0.4–31	0.3	8.2	0.2	2.8
194	$C_{16}H_{10}$	Pyrene	202.3	0.000	423.8	70.0	345–358	0.1–0.5	2.4	23.9	0.5	12.6
195	$C_{18}H_{12}$	Chrysene	228.3	0.699	531.2	1028.0	351–423	0.001–1.6	0.0	12.7	0.3	6.0
196	$C_{18}H_{12}$	Benzanthracene	228.3	0.000	433.6	14.4	352–434	0.01–25	0.4	18.8	0.5	8.1
197	$C_{18}H_{27}NO_3$	Capsaicin	305.4	0.000	510.8	67664.0	398–510[b]	0.01–62313[b]	0.1	2.3	0.0	1.3
198	$C_{18}H_{32}O_2$	Stearic acid	284.5	1.670	342.8	0.006	331–340[b]	0.001–0.01[b]	0.3	3.6	0.1	1.9
199	$C_{27}H_{46}O$	Cholesterol	386.7	1.721	421.7	0.75	325–421[b]	0.001–11[b]	0.3	3.8	−0.2	1.5
200	F_4Si	Silicon tetrafluoride	104.1	0.000	186.4	220730.0	130–186	200–220800	0.3	17.9	0.2	6.8
201	F_6S	Sulfur hexafluoride	146.1	0.000	223.2	232670.0	150–223	400–232700	0.9	12.6	0.5	8.4
202	$GaCl_3$	Gallium trichloride	176.1	5.096	350.9	1366.0	321–350[b]	133–1314[b]	0.4	3.2	0.0	1.4
203	H_2S	Hydrogen sulfide	34.1	0.968	187.7	23200.0	140–188	200–22700	1.7	16.2	0.3	4.4
204	HI	Hydrogen iodide	127.9	0.450	222.4	49326.0	160–222	200–49300	4.2	16.2	−2.5	11.6
205	Kr	Krypton	83.8	0.000	115.8	73154.0	80–116[b]	400–73100[b]	3.9	14.0	−1.8	9.7
206	NH_3	Ammonia	17.0	1.469	195.4	6111.0	160–195[b]	100–6120[b]	1.3	4.2	−0.1	2.7
207	NH_4Cl	Ammonium chloride	53.5	0.000	793.2	3500000.0	433–793	124–3327800	0.2	2.3	0.2	1.4
208	NO	Nitric oxide	30.0	0.153	109.5	21890.0	85–110	100–21900	0.6	15.0	−7.8	7.8
209	PH_3	Phosphine	34.0	0.570	139.4	3535.7	131–143	1333–5334	0.0	3.0	−0.8	0.8
210	S	Sulfur	32.1	0.000	388.4	3.1	323–388	0.03–4	1.4	13.3	0.3	7.1
211	$SbCl_3$	Antimony trichloride	228.1	3.927	346.6	723.7	298–346	18–719	0.4	4.8	0.1	2.2
212	Xe	Xenon	131.3	0.000	161.4	81668.0	110–161	300–81700	1.1	13.0	−1.8	7.1

[a] Taken from reference [26].

[b] Taken from reference [27].

the low values solid vapor pressure (below 0.001 Pa) for several carboxylic acids in the whole range of temperature. Also, substances with high variation of solid vapor pressure with temperature (such as neon and cyclohexane) to substances with low variation (such as silver and silicon dioxide) must be simultaneously considered by the network. In addition, the substances included in the study have very different physical and chemical characteristics. Low molecular weight substances such as carbon (M = 12) or methane (M = 16)

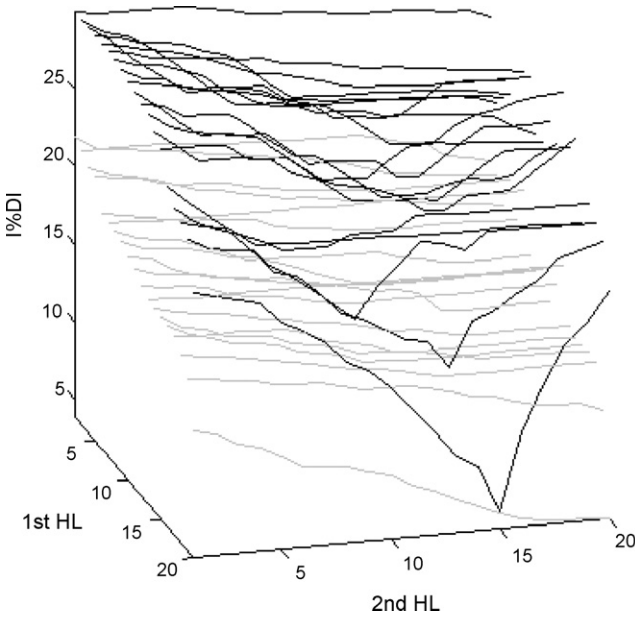

Fig. 2. Average absolute relative deviation found in correlating the solid vapor pressure of all substances as function of the number of neurons in the hidden layers (1st HL = first hidden layer, 2nd HL = second hidden layer). Grey line is the training error and black line is the prediction error.

to high molecular weight substances such as cholesterol (M = 387) or β-carotene (M = 537), or non-polar substances ($\mu = 0$) such as benzene, sulfur hexafluoride and xenon, to highly polar substances such as potassium iodide ($\mu = 9.2$), potassium chloride ($\mu = 10.3$) and glycine ($\mu = 12.8$) are part of the substances considered. Thus, the problem is not straightforward and probably is one of the reasons why the solid vapor pressure has not been treated using neural network as proposed in this paper.

Several network architectures were tested to select the most accurate. The accuracy was checked using the average relative deviation $\%\Delta P^S$ and average absolute deviation $|\%\Delta P^S|$ between the calculated value of P^S after training and the data from the literature.

Table 2
Overall minimum, maximum, and average deviations for the calculated solid vapor pressure for all the substances using the neural network model.

ANN model	$\%\Delta P^S_{\text{min}}$	$\%\Delta P^S_{\text{max}}$	$\%\Delta P^S$	$\|\%\Delta P^S\|$
Training set	0.00	26.41	0.22	4.84
Prediction set	0.00	−27.39	−0.29	5.03
Total set	0.00	−27.39	0.08	4.89

The deviations were calculated as:

$$\%\Delta P^S = \frac{100}{N}\sum_{i=1}^{N}\left[\frac{P^S_{\text{calc}} - P^S_{\text{lit}}}{P^S_{\text{lit}}}\right]_i \tag{5}$$

$$|\%\Delta P^S| = \frac{100}{N}\sum_{i=1}^{N}\left|\frac{P^S_{\text{calc}} - P^S_{\text{lit}}}{P^S_{\text{lit}}}\right|_i \tag{6}$$

Fig. 2 shows the average absolute relative deviation found in correlating the solid vapor pressure of all substances as function of the number of neurons in the hidden layers (1st HL = first hidden layer, 2nd HL = second hidden layer). The network that gave the lowest deviation during training was one with 5 neurons in the input layer, 20 and 15 neurons in the hidden layers, and one neuron in the output layer.

4. Results and discussion

The results are presented as the relative deviation $\%\Delta P^S$, the absolute deviation $|\%\Delta P^S|$, the minimum deviation, $\%\Delta P^S_{\text{min}}$ and the maximum deviation $\%\Delta P^S_{\text{max}}$ (Eqs. (5) and (6)). Table 1 presents the results. The last four columns in the Table show these deviations. Also shown at the end of the Table 1 are the deviations for the 62 substances used to check the prediction capabilities of the trained network. As observed in this table, the minimum, maximum, average and absolute average deviations for these substances are within the same ranges found during training.

Table 2 shows the overall minimum, maximum, and average deviations for all the substances using the proposed network 5-20-

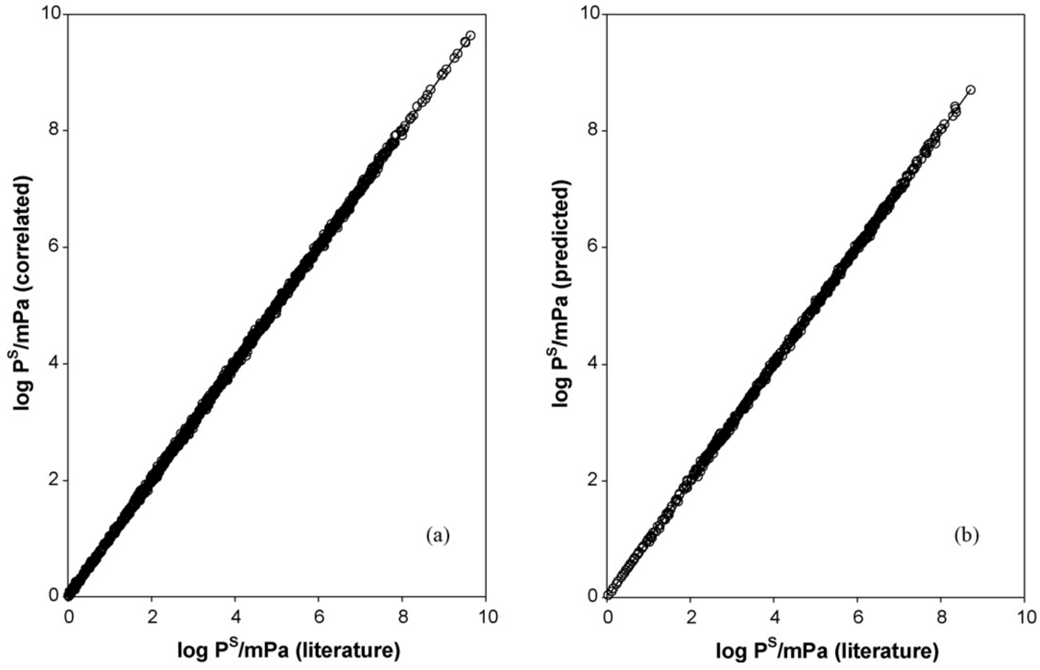

Fig. 3. Comparison between experimental and calculated values of the solid vapor pressure: (a) during training and (b) during prediction.

Table 3
Weights and biases of the 5-20-15-1 network.

w_{ij}	1	2	3	4	5	6	7	8	9	10	11	12	13	14	15	16	17	18	19	20
1	−0.6924	1.4748	1.1150	−1.9326	0.1552	0.5560	−0.6392	0.7832	−0.5316	2.8702	0.4137	−0.7350	0.1834	−0.1554	2.7805	0.9211	0.1522	8.9517	−1.6899	−0.7055
2	−4.2660	1.2580	−7.1784	−2.1381	7.7084	−2.4206	4.7676	5.4564	16.9890	−1.7208	−2.7257	−1.4163	−5.8151	4.2833	−13.313	5.0593	−4.4952	0.5271	0.9413	−1.7167
3	6.6955	−2.7893	3.3925	1.7563	−3.6261	6.2783	7.5138	−1.8996	−4.8416	−7.4996	9.3669	−9.6478	7.5579	−1.7612	0.1662	−8.4096	−0.1788	−2.0633	1.0730	−12.625
4	7.8172	0.4642	−4.0925	1.1421	−5.9928	0.6225	−3.4369	−3.6360	−0.4791	4.1322	−8.0065	9.1037	−0.2293	1.3348	5.9353	−10.319	−1.8094	−0.1869	−4.9576	0.5897
5	−9.2963	0.1984	6.9873	−1.0866	−0.6739	−6.3154	−6.5740	0.1030	−3.1064	2.3006	1.9355	−1.2141	5.8806	−2.6250	2.4534	−6.1613	−10.072	−0.6445	3.3928	5.4948
b_j	−6.7628	−0.4444	3.0448	0.1304	2.7843	−1.4295	4.4618	3.1556	9.9103	0.2693	5.6905	−6.4927	5.4491	1.0076	−4.6665	−7.6898	−11.526	7.8351	−0.8259	−8.9110

w_{kj}	1	2	3	4	5	6	7	8	9	10	11	12	13	14	15	16	17	18	19	20	b_k
1	−7.3905	2.6655	4.6043	0.2572	−9.0951	16.350	11.923	4.9596	−3.2280	2.7695	7.8625	−5.6063	−9.8188	4.2191	−4.8660	−3.3821	−7.5293	14.2210	−2.4146	4.2374	1.4764
2	7.8847	0.5827	1.5886	2.7575	−2.3979	−0.1195	1.8688	3.2768	−3.5676	3.0063	−1.2019	0.8608	−6.1543	−0.8756	−2.3629	3.7808	−1.2401	2.8977	−1.4956	−0.5817	1.1731
3	5.4681	0.4577	1.9602	2.8028	−5.1551	−0.5376	2.4783	2.6878	2.5539	−1.1361	0.0549	2.8213	0.0575	0.8874	−0.4283	5.9295	−2.4705	2.7386	1.0089	2.8238	−0.9245
4	4.0401	2.1060	3.1305	−3.5958	5.3676	−0.9117	1.5109	−6.5559	−6.7700	3.0399	0.8897	−1.2095	−3.4133	2.7887	−2.4468	−0.7564	1.5716	3.4019	−1.4920	2.8855	−1.6608
5	−0.1315	−0.1465	4.6775	−1.9695	−0.4531	−2.4794	−0.4534	−5.3252	−6.4532	−5.0016	−0.7837	−3.3365	−1.9114	2.5493	−0.2468	4.1329	1.2177	5.2986	−2.2792	−2.2091	−4.1477
6	1.0368	0.3491	1.8390	1.2721	−0.4492	−5.5863	−1.6839	4.2807	2.4783	−5.4142	−1.0474	1.0393	1.6171	−0.6768	3.0104	−0.5012	−2.6722	6.7812	−5.2218	−1.5158	0.4099
7	−5.0198	−1.5233	3.4707	−2.8133	6.2743	−7.9386	2.9012	−11.270	−2.8383	4.6444	−3.9408	1.5686	1.6506	−3.9802	−2.4288	1.0849	−2.3655	−4.5535	0.9387	−14.495	3.1864
8	1.8816	0.5584	4.2591	−0.8034	2.1574	1.8377	0.1361	−4.3579	6.6180	1.3788	−0.7546	−3.1747	−0.6054	2.8310	0.5456	−0.7356	−2.3066	−0.4040	2.5352	4.9286	−1.8166
9	−0.8297	−3.0518	2.2891	0.7644	−6.4947	2.6269	0.7936	5.8249	−1.0313	−2.4662	3.0216	−1.5472	4.6165	6.0064	1.6699	0.9635	0.9656	−3.0207	0.8563	0.7016	1.8331
10	−2.6724	−1.0735	2.9131	0.4630	0.2659	2.1532	4.4726	2.4711	2.9340	5.1857	−2.1507	−0.1838	−1.1729	1.0782	0.9344	−1.4404	3.2118	−0.0989	0.4782	−0.1103	3.8623
11	1.0521	1.8930	−0.7765	3.2980	3.5104	1.3049	−0.6828	−2.7208	5.2032	0.7500	−3.6193	−5.0624	−0.6169	1.9190	−0.3028	−2.2168	−1.6394	−2.6579	1.6730	4.0764	1.6036
12	−1.4926	3.7789	−5.0190	2.7957	3.2334	0.8573	0.9790	−0.3709	0.3399	−0.1262	0.7389	−0.5232	1.4848	−4.0331	0.1936	−1.0113	−0.9202	−2.1908	0.2926	0.3232	−1.5699
13	0.2215	0.6154	−5.9007	1.5848	−2.5277	1.1424	−1.2666	2.4404	0.6628	1.4810	1.0360	0.4384	12.6100	−2.0339	0.0639	1.2424	1.2312	−2.8517	1.0740	0.1039	−6.5020
14	−0.5835	−0.8920	0.4162	0.4613	4.4767	−2.4462	−3.8262	−1.3560	−1.5749	0.1397	−4.1398	−2.2892	−0.6108	5.8177	0.6193	2.4288	5.5953	−3.1987	2.8629	−2.5188	−1.9047
15	−0.7787	−2.7696	0.0956	−2.4172	−1.0470	4.0493	2.4703	2.7280	4.6704	−0.4902	−3.2340	3.2410	2.0171	−9.3889	−0.0172	−0.3384	−0.9102	−2.1303	−3.2038	2.6201	0.2988

w_{lk}	1	2	3	4	5	6	7	8	9	10	11	12	13	14	15	b_l
1	0.8170	3.1649	2.6393	−6.6692	2.5623	19.889	−5.0096	12.743	−6.4043	−12.749	−10.990	8.9176	−9.8282	−5.9996	−4.7430	−5.3776

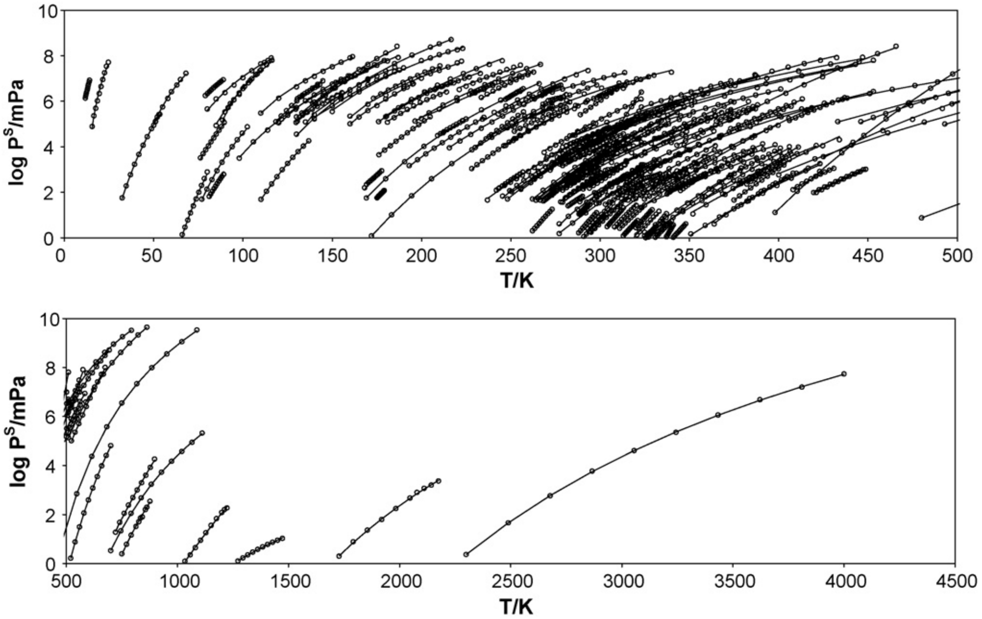

Fig. 4. Solid vapor pressures for all substances considered in the study. The circles are the results of the ANN while the solid lines are literature values.

15-1. The results show that the ANN can be accurately trained and that the chosen topology can estimate the solid vapor pressure with acceptable accuracy (absolute average deviations less than 5% for training and average deviations of less than 5% for the 62 substances used in the prediction step).

Once the best architecture was determining, the optimum weights required to carry out the estimate of the pressure of solid vapor of any substance, were obtained. Table 3 shows the optimum weight and biases for the multilayer neural network 5-20-15-1.

Table 4 presents a comparison between some methods proposed in the literature and the method proposed in this work. The low deviations found with the proposed method indicate that the trained ANN can estimate the solid vapor pressure with better accuracy than other methods. Neau et al. [1] with the use of the Peng–Robinson equation of state and Coutsikos et al. [2] using a group contribution method predicted solid vapor pressures with average absolute deviations higher than 20% and maximum deviations grater than 70%. The predictions with the proposed network show average absolute deviations below 5% and maximum deviations are a little higher than 15%. These results represent a tremendous increase in accuracy for predicting this important property and show that not only the use of the optimum network architecture is crucial, but also the appropriate selection of the independent variables (M, μ, T_{TP}, P_{TP}, and $P^S \to 0$ as $T \to 0$).

Fig. 3 shows a comparison between experimental (solid line) and calculated values (points) of the solid vapor pressure. Fig. 3a shows a comparison during training between correlated and literature values of the solid vapor pressure. The correlation coefficient R^2 is 0.9998 and the slope of the curve (expected to be 1.0) is 0.9996. Fig. 3b shows a comparison during prediction between predicted and literature values of the solid vapor pressure. In this case, the correlation coefficient R^2 is 0.9997 and the slope of the curve (also expected to be 1.0) is 1.0003. Fig. 4 presents the calculated values (circles) and the literature values (solid line) for the solid vapor pressure for all substances included in the study. This figure, on the other hand allows to get a general picture of the ranges of temperature and solid vapor pressures that have been considered in the study.

Table 4
Comparison of the method proposed in this work with other methods found in the literature to determine the solid vapor pressure.

Method	No. of substances	No. of data point	$\lvert\%\Delta P^S\rvert_{\min}$	$\lvert\%\Delta P^S\rvert_{\max}$	$\lvert\%\Delta P^S\rvert$
Neau et al. [1]	22	259	4.60	87.40	22.80
Coutsikos et al. [2]	212	2774	2.00	74.00	26.73
This work	212	2120	0.43	15.30	4.89

5. Conclusions

Based on the results and discussion presented in this study, the following main conclusions are obtained: (i) The great differences in structure, chemical and physical properties of the substances considered in the study impose additional difficulties on the problem that the proposed ANN has been able to handle. (ii) The results show that the ANN can be properly trained and that the chosen topology (5-20-15-1) can estimate the solid vapor pressure with acceptable accuracy. (iii) The upper and lower ends of the sublimation curve (T_{TP}, P_{TP} and $P^S \to 0$ as $T \to 0$), have influential effects on the good training and predicting capabilities of the chosen network.

Acknowledgement

The author thank at Department of Physics of the University of La Serena-Chile by special support that made possible the preparation of this paper.

References

[1] E. Neau, S. Garnier, L.A. Avaullée, Fluid Phase Equilib. 164 (1999) 173–186.
[2] P. Coutsikos, E. Voutsas, K. Magoulas, D.P. Tassios, Fluid Phase Equilib. 207 (2003) 263–281.
[3] T.Y. Kwak, G.A. Mansoori, Chem. Eng. Sci. 41 (1986) 1303–1309.
[4] J.O. Valderrama, Ind. Eng. Chem. Res. 42 (2003) 1603–1618.
[5] A.H. Jones, J. Chem. Eng. Data 5 (1960) 196–200.
[6] C.A. Faúndez, J. Díaz-Valdés, J.O. Valderrama, Thermochim. Acta 462 (2007) 25–31.
[7] J.S. Chickos, R. Sabbah, S. Hosseini, J.F. Liebman, Struct. Chem. 7 (1996) 391–395.
[8] J.S. Chickos, W.E. Acree, J. Phys. Chem. Ref. Data 31 (2002) 537–698.
[9] A. Vetere, Fluid Phase Equilib. 148 (1998) 83–93.
[10] Y. Iwai, M. Yamamoto, Y. Hata, Y. Koga, Y. Arai, J. Chem. Eng. Jpn. 29 (1996) 728–731.
[11] F. Trabelsi, K. Abaroudi, F. Recasens, J. Supercrit. Fluids 14 (1999) 151–161.
[12] X. Nanping, W. Zhoohui, D. Junhang, S. Jun, Chin. J. Chem. Eng. 5 (1997) 29–37.

[13] B.T. Goodman, W.V. Wilding, J.L. Oscarson, R.L. Rowley, Int. J. Thermophys. 25 (2004) 337–350.
[14] M.L. Cygnarowicz, R.J. Maxwell, W.D. Seider, Fluid Phase Equilib. 59 (1990) 57–71.
[15] E. Reverchon, G. Della Porta, R. Taddeo, Ind. Eng. Chem. Res. 34 (1995) 4087–4091.
[16] P. Subra, S. Castellani, H. Ksibi, Y. Gabarros, Fluid Phase Equilib. 131 (1997) 269–286.
[17] J.O. Valderrama, J. Zavaleta, Ind. Eng. Chem. Res. 44 (2005) 4824–4833.
[18] J.A. Lazzús, J. Taiwan Inst. Chem. Eng. 40 (2009) 213–232.
[19] J. Taskinen, J. Yliruusi, Adv. Drug Deliv. Rev. 59 (2003) 1163–1183.
[20] D. Yaffe, Y. Cohen, J. Chem. Inf. Comput. Sci. 41 (2001) 463–477.
[21] G. Espinosa, D. Yaffe, A. Arenas, Y. Cohen, F. Giralt, Ind. Eng. Chem. Res. 40 (2001) 2757–2766.
[22] G. Espinosa, D. Yaffe, Y. Cohen, A. Arenas, F. Giralt, J. Chem. Inf. Comput. Sci. 40 (2000) 859–879.
[23] B. Diu, C. Guthmann, D. Lederer, B. Roulet, Eur. J. Phys. 23 (2002) 205–212.
[24] G. Ding, J. Chen, X. Qiao, L. Huang, J. Lin, X. Chen, Chemosphere 62 (2006) 1057–1063.
[25] M. Karelson, V.S. Lobalov, A.R. Katritzky, Chem. Rev. 96 (1996) 1027–1044.
[26] T.E. Daubert, R.P. Danner, H.M. Sibul, C.C. Stebbins, Physical and Thermodynamic Properties of Pure Chemicals. Data Compilation, Taylor & Francis, London, 2000.
[27] R.C. Weast, M.J. Astle, CRC Handbook of Chemistry and Physics: A Ready-Reference Book of Chemical and Physical Data, 61st ed., Chemical Rubber Company, Florida, 1980, p. C-583.
[28] S. Chattopadhyay, P.J. Ziemann, Aerosol Sci. Tech. 39 (2005) 1085–1100.